www.lpr-journal.org

LASER & PHOTONICS REVIEWS

WILEY-VCH

Laser Photonics Rev. **7,** No. 6, L93–L97 (2013) / **DOI** 10.1002/lpor.201300112

LASER & PHOTONICS REVIEWS

Abstract Five-cycle (50 fs) mid-IR pulses at 80-MHz repetition rate are produced using a degenerate (subharmonic) optical parametric oscillator (OPO), synchronously pumped by an ultrafast 1560-nm fiber laser. The effects of cavity dispersion and the length of a periodically poled lithium niobate (PPLN) gain element on the output spectrum and pulse duration are investigated by taking advantage of a very broad ($\sim$ 1000 cm^{-1}) gain bandwidth near the 3.1-μm OPO degeneracy point. A new method of assessing the total OPO group delay dispersion across its entire spectrum is proposed, based on measuring spectral signatures of trace amounts of molecular gases injected into the OPO cavity.

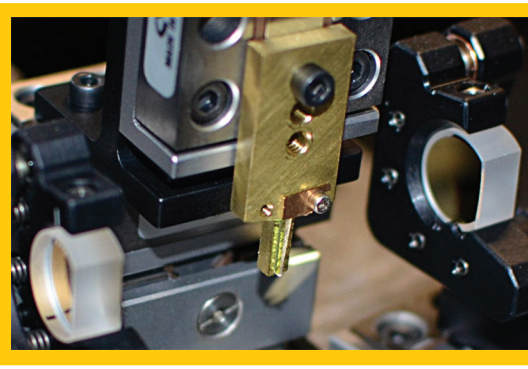

LETTER ARTICLE

Five-cycle pulses near $\lambda = 3$ μm produced in a subharmonic optical parametric oscillator via fine dispersion management

Magnus W. Haakestad[1], Alireza Marandi[2], Nick Leindecker[2], and Konstantin L. Vodopyanov[3,*]

1. Introduction

Laser sources producing phase-stabilized few-cycle pulses in the mid-IR (>2.5 μm) region have important applications such as high-harmonic generation, attosecond science, pump-probe spectroscopy, and as frequency comb sources for precision and ultrasensitive molecular detection [1, 2]. Several approaches for generating few-cycle mid-IR pulses have been demonstrated, based on three- and four-wave mixing processes [3–6]. Common to these approaches is that the repetition rate is typically limited to the kHz range. Few-cycle pulses at 49 MHz repetition rate and ~1-mW average power were produced in a two-branch Er:fiber laser system based on frequency shifting in a highly nonlinear silica fiber and subsequent difference frequency mixing [7]. Here we produce few-cycle mid-IR pulses at 80 MHz repetition rate with ~40 mW average power based on a sync-pumped degenerate OPO [8–10], and optimize the output by varying the round-trip dispersion and nonlinear crystal length.

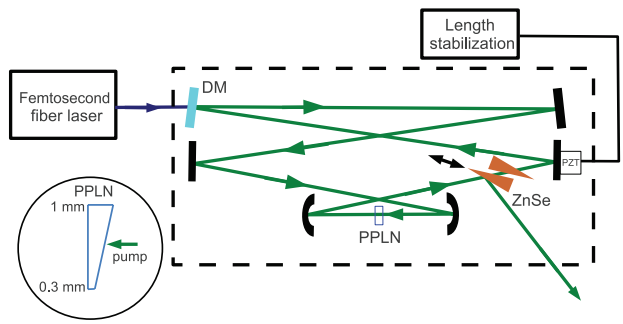

Figure 1 Schematic of the degenerate broadband OPO. The pump beam is introduced through the in-coupling dielectric mirror DM. The other five mirrors are gold coated. A pair of wedges made of ZnSe is used for dispersion compensation and beam out-coupling. The PPLN crystal (inset) is AR-coated and has a 4-degree wedge for continuous adjustment of crystal length from 0.3–1.0 mm. PZT is a piezo actuator for cavity length control. The OPO is kept in a Plexiglas enclosure (dotted line), which is flushed with N_2.

2. Experiments

The OPO is pumped by an Er:fiber laser (Toptica FemtoFiber pro IR, 350 mW average power, 1.56 μm wavelength, $f_{rep} = 80$ MHz repetition rate, 85 fs pulse duration). It is doubly resonant and operates near 3.1-μm degeneracy. The setup (Fig. 1) is similar to that of Ref. [11], except for one important difference that here, the MgO-doped PPLN crystal, with domain reversal period of 34.8 μm, is in the form of an antireflection-coated 4-degree wedge, allowing for continuous tuning of the PPLN length from 0.3–1.0 mm by translating the crystal perpendicular to the pump. In addition, a pair of 1-degree ZnSe wedges near Brewster's angle is used for dispersion compensation and beam out-coupling.

It is well known that extra wide phase-matching bandwidth can be obtained by operation at degeneracy, where the co-polarized signal and idler have identical group

[1] Norwegian Defense Research Establishment (FFI), P O Box 25, NO-2027 Kjeller, Norway
[2] E. L. Ginzton Laboratory, Stanford University, Stanford, CA 94305, USA
[3] Univ. Central Florida, CREOL, College of Optics & Photonics, Orlando, FL 32816, USA
*Corresponding author: e-mail: vodopyanov@creol.ucf.edu

velocity in the nonlinear crystal. In this case, the phase-matching bandwidth is approximately

$$\Delta\nu \approx \frac{1}{\sqrt{\pi|\beta_2|L}}, \qquad (1)$$

where β_2 is the group velocity dispersion (GVD, $d^2k/d\omega^2$) of the nonlinear crystal at the OPO center frequency and L is its length. For a given nonlinear crystal it is thus optimal to pump near half the zero-GVD wavelength (near 1.0 μm for PPLN), as in Ref. [10], to obtain the broadest phase-matching bandwidth. However, when pumped at 1.56 μm, the phase-matching bandwidth of PPLN is still sufficiently wide ($\Delta\nu/\nu = 0.45 - 0.25$ for 0.3 to 1 mm-long PPLN) to obtain few-cycle pulses in the important 3-μm region.

To minimize the group delay dispersion (GDD) effects, we were able to tune the zero-GDD wavelength of the cavity by translating the ZnSe wedges. Figure 2(a) shows the contributions to the total round-trip dispersion for the configuration that gave the shortest pulses (0.8 mm PPLN and 2.2 mm ZnSe). We observe that the GDD at the central OPO wavelength of 3.12 μm is slightly negative in this case (-97 fs^2), with third-order dispersion dominating across the phase-matching bandwidth (2.6–3.8 μm).

Two conditions are necessary to get oscillation in our special case of a degenerate OPO: (i) The sync-pumping condition, i.e. the round-trip time of the cavity must match the repetition period of the pump laser. (ii) Since the signal and idler combs merge into one comb of subharmonic frequencies, the additional constraint $f_{\mathrm{ceo,signal}} = f_{\mathrm{ceo,idler}}$ allows only the values $f_{\mathrm{ceo,pump}}/2$ and $\left(f_{\mathrm{ceo,pump}} + f_{\mathrm{rep}}\right)/2$ for the subharmonic comb's carrier-envelope offset (CEO) frequency. The result is (inset to Fig. 2(b)) that the OPO only resonates at a discrete set of cavity lengths separated (in round-trip) by approximately one pump wavelength [11].

In our experiment, the OPO cavity length was locked to one of the resonances using a servo loop and a PZT actuator [11] (Fig. 1). In general, the intracavity dispersion can not be totally compensated over the whole range of OPO frequencies, and thus the OPO comb lines acquire an extra phase delay $\Delta\phi$ per roundtrip and the electric-field amplitude roundtrip transmission t becomes complex: $E \rightarrow tE; t = \exp(-\delta_0 - i\Delta\phi)$ [12]. Here δ_0 is the roundtrip field loss in the cavity. The tolerance to the roundtrip phase shift is determined by the cavity finesse and nonlinear gain [8].

Figure 2(b) shows calculated phase shifts $\Delta\phi$ for three neighboring resonance peaks with respect to cavity length, assuming 0.8-mm PPLN and 2.2-mm ZnSe. Changing the cavity length between discrete neighboring values changes a tilt in the $\Delta\phi$ vs. frequency dependence.

For each combination of PPLN/ZnSe lengths (varied in the range 0.3–0.8 mm and 0.7–3.4 mm, respectively) the OPO spectrum and corresponding 2nd order autocorrelation signal was measured for each oscillation peak. For spectral measurements, we have used scanning Michelson interferometry based on a commercial Nicolet 6700 spectrometer, and for the 2-nd order interferometric autocorrelation measurements we used two-photon detection with an InGaAs photodetector in collinear geometry. In qualitative agreement with Fig. 2(b), we found that the OPO spectrum was single-peaked for positive cavity length detunings, and became double-peaked for negative detunings. Figure 2(c) plots the measured spectra for three neighboring oscillation peaks (No. 2–4) obtained with 0.8-mm PPLN and 2.2-mm

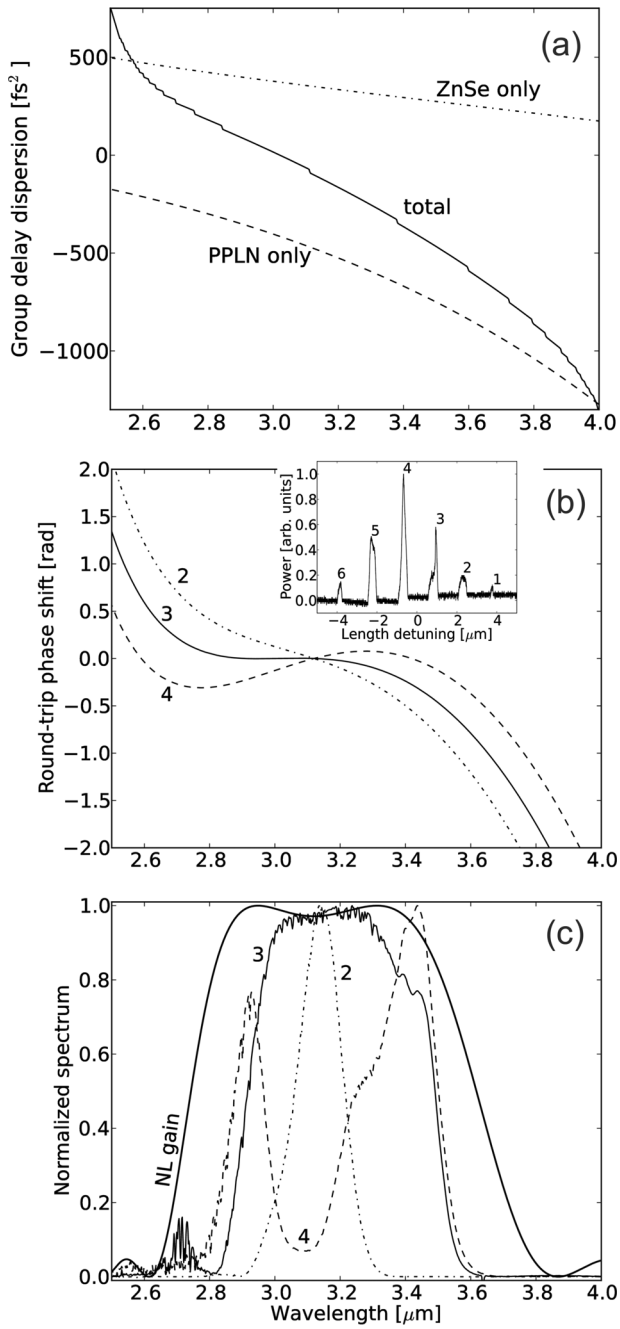

Figure 2 (a) Calculated GDD for 0.8-mm PPLN and 2.2-mm ZnSe, respectively. Also shown is the total cavity round-trip GDD, including the contribution from the dielectric mirror. (b) Estimated round-trip phase shift for three neighboring cavity-length peaks (No. 2–4) shown in the inset. (c) Measured output spectra with 0.8 mm PPLN and 2.2 mm ZnSe for peaks 2–4. Also shown is the calculated parametric gain curve for 0.8-mm PPLN.

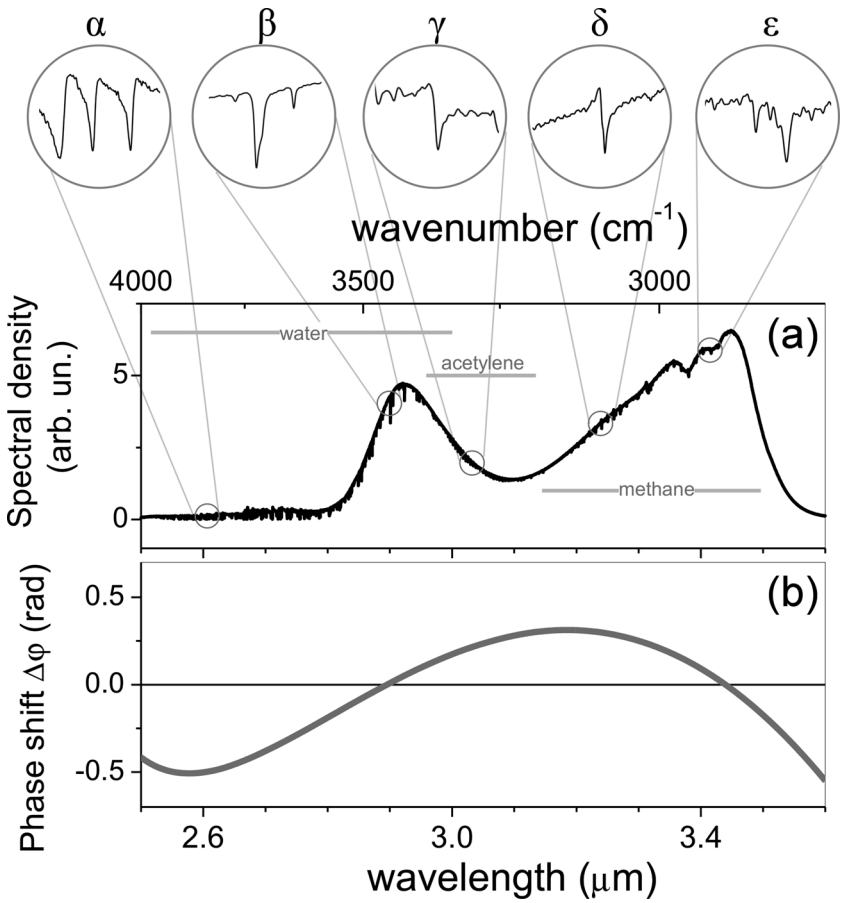

Figure 3 Mapping the OPO cavity dispersion. (a) Experimentally measured OPO spectrum (0.8 mm PPLN, 1.5 mm ZnSe) containing absorption features of trace amounts of methane, acetylene and water vapor inside the cavity and serving as a probe for dispersion. Comparing shapes of peaks α–ε, one can see the dispersive nature of peaks α, γ, δ, corresponding to non-zero roundtrip extra phase $\Delta\phi$. (b) Round-trip phase shift $\Delta\phi(\nu)$ retrieved by polynomial fitting.

ZnSe. The broadest single-peaked OPO spectrum is obtained with peak No. 3 at the average output power up to 40 mW. For a too long cavity (peak No. 2), only a small spectral region close to degeneracy has a sufficiently small roundtrip extra phase shift. On the other hand, for a too short cavity (peak No. 4), the OPO may become non-degenerate, that is the spectrum splits into two distinct (signal and idler) combs with, generally speaking, different f_{CEO} [13]. We observed that the spectral- and autocorrelation shapes could drift over timescales of several minutes, and attribute this to drift of the CEO frequency of the free running pump laser. Since the OPO cavity was actively locked to double resonance, small variations in f_{ceo} of the pump were tracked by the electronic servo loop and were compensated by small (sub-μm scale) adjustments of the OPO cavity length. This caused small changes in the slope of the round-trip phase shift, which affected the OPO spectrum.

We discovered that the cavity $\Delta\phi$ (and thus cavity GDD, $d^2\Delta\phi/d\omega^2$) can be mapped across the OPO spectrum by injecting small amounts of known gases into the cavity. Due to mutual action of the cavity phase shift and refractive index change near molecular resonance (antisymmetric with respect to the line center), the absorption line shape acquires Fano resonance-like features [12]. Physically, an additional phase shift caused by a molecular resonance, reduces, on one side of the absorption peak, and increases, on the other side of the peak, the mismatch between the OPO frequency comb lines and the OPO cavity resonances (we assume that the OPO mode spacing is smaller than the molecular absorption line width). This causes asymmetry of the spectral line shapes, by measuring which and comparing them to a database, we were able, taking into account that the phase shift is a slow function of frequency, to map $\Delta\phi$ in the whole range of OPO frequencies [12].

Figure 3 illustrates the process of intracavity dispersion mapping. An experimentally measured OPO spectrum with trace amounts of methane, acetylene and water vapor injected into the cavity is shown in Fig. 3(a). Comparing spectral shapes of the peaks α–ε, one can see that peaks α, γ, and δ show strong derivative (Fano-type) features. For α, the sign of the derivative-like component of spectral dips is opposite to that of γ and δ, indicating $\Delta\phi < 0$ in the former, and $\Delta\phi > 0$ in the latter cases [12]. Figure 3(b) plots the retrieved round-trip phase shift $\Delta\phi(\nu)$, which is consistent with the known GDD of the intracavity elements.

Knowing $\Delta\phi$ vs ν allows us to estimate the absolute spectral phase ϕ of the out-coupled beam (defined by $A(\nu) = |A(\nu)| \exp[i2\pi\nu t + i\phi(\nu)]$) across the OPO spectrum. The procedure is as follows: In Ref. [12], we expressed the complex form of the stationary OPO electric field spectral amplitude $A(\nu)$ as

$$A(\nu) = \frac{\Delta A}{1 - \exp(-\delta_0 - i\Delta\phi)} \approx \frac{\Delta A}{\delta_0 + i\Delta\phi}, \qquad (2)$$

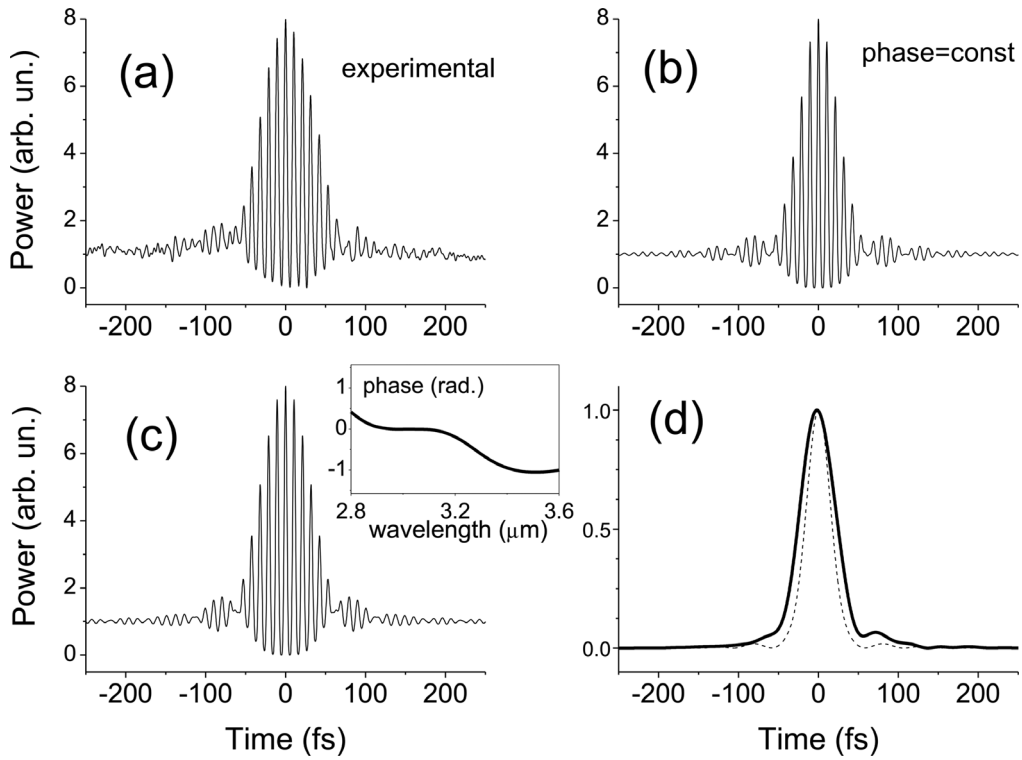

Figure 4 (a) Measured autocorrelation. (b) calculated transform-limited autocorrelation. (c) calculated autocorrelation using estimated spectral phase (inset). (d) estimated pulse shape (solid line, FWHM duration 51 fs) and transform-limited pulse shape (dotted line, FWHM duration 35 fs).

where ΔA is the slowly varying nonlinear optical gain, due to the presence of the pump, and δ_0 is the cavity roundtrip field loss, measured to be $\delta_0 \approx 0.14$ (25% roundtrip power loss). Since we know δ_0 and $\Delta\phi$, we can extract the absolute phase ϕ as:

$$\phi \approx \arg\left[1/(\delta_0 + i\,\Delta\phi)\right]. \qquad (3)$$

In the limit when $|\Delta\phi| \ll \delta_0$, the effect of the cavity round-trip extra phase delay is enhanced, due to multipass action, by a factor $1/\delta_0$, similar to the enhancement of the intracavity absorption observed in Ref. [12].

Figure 4(a) shows the measured autocorrelation signal for peak No. 3 in Fig. 2(c). This combination of PPLN length, ZnSe length and peak No. gave the shortest clean autocorrelation signal. In this case a 2.5-mm-thick slab of ZnSe was inserted after the OPO to minimize the wings of the autocorrelation signal. The corresponding calculated transform-limited (i.e. with constant spectral phase) autocorrelation signal is shown in Fig. 4(b). Using Eq. (3) to estimate the spectral phase from the OPO (inset to Fig. 4(c)) and taking the dispersion of the autocorrelator (~ 500 fs^2 at 3.1 μm) and the external ZnSe slab into account, we obtain the calculated autocorrelation in Fig. 4(c). The respective calculated intensity shape is shown in Fig. 4(d), which has a FWHM duration of 51 fs (4.9 optical cycles). The transform-limited pulse would have had a duration of 35 fs (3.4 cycles).

3. Conclusions

In conclusion, we have demonstrated that a degenerate sync-pumped OPO can generate few-cycle ($\sim$ 50 fs) 3-μm pulses with predictable, based on mapping of intracavity dispersion with molecular spectral signatures, spectral phase characteristics. Since the mid-IR pulses are phase-locked to the pump laser [14], an f_{CEO}-stabilized pump would automatically lead to phase-stabilized mid-IR output. The pulse duration achieved was limited mostly by the uncompensated 3rd order dispersion in the OPO cavity. Shorter pulses (down to 2–3 cycles) can be achieved by GDD compensation with dispersive mirrors.

Acknowledgements. We acknowledge financial support by the US Office of Naval Research, NASA, Air Force Office of Scientific Research, Agilent Technologies, Stanford Medical School, Stanford Woods Institute, and Sanofi Aventis. We are indebted to Tobias P. Lamour for assistance with measuring intracavity spectra. MWH acknowledges Gunnar Arisholm for his comments on the manuscript.

Received: 2 August 2013, **Revised:** 27 August 2013, **Accepted:** 16 September 2013

Published online: 8 October 2013

Key words: Ultrafast nonlinear optics, optical parametric oscillators, periodically-poled lithium niobate, mid-infrared.

References

[1] A. Schliesser, N. Picqué, and T. W. Hänsch, Nature Phot. **6**, 440–449 (2012).
[2] S. A. Diddams, J. Opt. Soc. Am. B **27**, B51–B62 (2010).
[3] D. Brida, M. Marangoni, C. Manzoni, S. D. Silvestri, and G. Cerullo, Opt. Lett. **33**(24), 2901–2903 (2008).
[4] O. Chalus, A. Thai, P. K. Bates, and J. Biegert, Opt. Lett. **35**(19), 3204–3206 (2010).
[5] C. Heese, C. R. Phillips, B. W. Mayer, L. Gallmann, M. M. Fejer, and U. Keller, Opt. Express **20**(24), 26888–26894 (2012).
[6] T. Fuji and T. Suzuki, Opt. Lett. **32**(22), 3330–3332 (2007).
[7] A. Sell, R. Scheu, A. Leitenstorfer, and R. Huber, Appl. Phys. Lett. **93**, 251107 (2008).
[8] S. T. Wong, K. L. Vodopyanov, and R. L. Byer, J. Opt. Soc. Am. B **27**, 876–882 (2010).
[9] N. Leindecker, A. Marandi, R. L. Byer, K. L. Vodopyanov, J. Jiang, I. Hartl, M. Fermann, and P. G. Schunemann, Opt. Express **20**, 7046–7053 (2012).
[10] C. W. Rudy, A. Marandi, K. A. Ingold, S. J. Wolf, K. L. Vodopyanov, R. L. Byer, L. Yang, P. Wan, and J. Liu, Opt. Express **20**(25), 27589–27595 (2012).
[11] N. Leindecker, A. Marandi, R. L. Byer, and K. L. Vodopyanov, Opt. Express **19**, 6296–6302 (2011).
[12] M. W. Haakestad, T. P. Lamour, N. Leindecker, A. Marandi, and K. L. Vodopyanov, J. Opt. Soc. Am. B **30**, 631–640 (2013).
[13] K. F. Lee, J. Jiang, C. Mohr, J. Bethge, M. E. Fermann, N. Leindecker, K. L. Vodopyanov, P. G. Schunemann, and I. Hartl, Opt. Lett. **38**(8), 1191–1193 (2013).
[14] A. Marandi, N. C. Leindecker, V. Pervak, R. L. Byer, and K. L. Vodopyanov, Opt. Express **20**(7), 7255–7262 (2012).